PLOS ONE

RESEARCH ARTICLE

Nicotinic receptor components of amyloid beta 42 proteome regulation in human neural cells

Patricia Sinclair[1], **Nadine Kabbani**[1,2]*

1 Interdisciplinary Program in Neuroscience, George Mason University, Fairfax, VA, United States of America, **2** School of System Biology, George Mason University, Fairfax, VA, United States of America

* nkabbani@gmu.edu

Citation: Sinclair P, Kabbani N (2022) Nicotinic receptor components of amyloid beta 42 proteome regulation in human neural cells. PLoS ONE 17(8): e0270479. https://doi.org/10.1371/journal.pone.0270479

Editor: Wataru Araki, National Center of Neurology and Psychiatry (NCNP), JAPAN

Received: February 15, 2022

Accepted: June 12, 2022

Published: August 12, 2022

Data Availability Statement: All relevant data are within the article and its Supporting Information files.

Funding: The study was supported by an Alzheimer's and Related Diseases Research Award Fund (ARDRAF) grant to NK. The funders had no role in study design, data collection and analysis, decision to publish, or preparation of the manuscript.

Competing interests: The authors have declared that no competing interests exist.

Abstract

Alzheimer's disease (AD) is associated with chronic neurodegeneration often accompanied by elevated levels of the neurotoxic peptide amyloid-beta 1–42 ($A\beta_{42}$) in the brain. Studies show that extracellular $A\beta_{42}$ binds to various cell surface receptors including the human α7 nicotinic acetylcholine receptor (nAChR) and activates pathways of neurotoxicity leading to cell death. The α7 nAChR is thus considered a promising drug target for therapy against neurodegenerative disease such as AD. In this study, we use mass spectrometry-based label-free precursor ion quantification to identify proteins and pathways that are changed by a 72-hour treatment with $A\beta_{42}$ or $A\beta_{42}$ in the presence of the α7 nAChR blocker, α-bungarotoxin (Bgtx) in the human neuroblastoma SH-SY5Y cell line. Bioinformatic gene ontology enrichment analysis was used to identify and characterize proteins and pathways altered by $A\beta_{42}$ presentation. The results support evidence on the involvement of mitochondrial proteins in $A\beta_{42}$ responses and define potential mechanisms of α7 nAChR mediated amyloid toxicity. These findings can inform pharmacological strategies for drug design and treatment against amyloid disease.

Introduction

Extracellular amyloid plaques and intracellular tangles of hyperphosphorylated tau are physiological hallmarks of Alzheimer's disease (AD) used to confirm diagnosis during post-mortem examination of brain tissue [1]. While much remains unknown about the etiology and cellular pathology underlying AD, insight from genetic predisposing factors suggest that AD may arise from variability in lipid and protein processing within neural cells. In particular, mutations in genes for amyloid precursor protein (APP) and its processing favor increased generation of the pathogenic amyloid-beta 1–42 ($A\beta_{42}$) peptide and confer susceptibility to early onset AD [2]. The self-assembly of $A\beta_{42}$, which is seen both *in vivo* and *in vitro*, leads to the formation of higher order amyloid structures (e.g. oligomers) which appear to drive disrupted signaling in cells and brain tissue [3]. Studies show that $A\beta_{42}$ can critically drive membrane calcium signaling, disrupt intracellular protein trafficking and degradation, and increase mitochondrial oxidative stress in various types of neural cells [4].

AD degeneration appears early in the cholinergic neurons of the basal forebrain and impacts projections to regions such as the entorhinal cortex [5]. Various components of the cholinergic system, including nicotinic acetylcholine receptors (nAChR) are expressed in these basal forebrain neurons and have been implicated in amyloid neurotoxicity [6, 7]. Studies show that $A\beta_{42}$ can directly bind the α7 nAChR within the orthosteric ligand binding site thus altering calcium entry into neurons [8–10]. In addition to calcium signaling, α7 nAChRs are known to activate several downstream signaling pathways and regulate cytoskeletal and mitochondrial activity [9, 10]. In SH-SY5Y cells oligomeric $A\beta_{42}$ peptide was found to mediate a robust inhibition of ERK phosphorylation induced by choline activation of α7 nAChRs [11]. Targeting the α7 nAChR has been suggested as an important strategy for drug development against AD and other neuro-disorders [12, 13].

In recent work we profiled responses to $A\beta_{42}$ within the proteome of nerve growth factor (NGF) differentiated pheochromocytoma 12 (PC12) cells using tandem mass spectrometry-based label-free quantitative analysis coupled to bioinformatics [14]. Here, we extend this approach to determine the impact of $A\beta_{42}$ in the human neuroblastoma SH-SY5Y cell line, which is an established model for the study of amyloid processing [15, 16]. We begin to explore the involvement of α7 nAChRs in $A\beta_{42}$ neurotoxicity by comparing proteome responses in cells treated with $A\beta_{42}$ in the presence or absence of the α7 nAChR blocker Bgtx.

Methods and materials

Cell culture and drug treatment

Human neuroblastoma cells SH-SY5Y cells (ATCC® CRL-2266™) were grown in DMEM (Gibco 11995065) supplemented with 10% fetal bovine serum (FBS) and 1% pen/strep in T75 cell culture treated flasks at 37˚C and 5% CO2. Passage 10 cells grown to 70% confluence were treated with 100 nM $A\beta_{42}$ (Bachem, H-6466) or its reverse, amyloid-beta 42–1, ($A\beta_{rev}$) (Bachem, H-3976) prepared as described in Arora et al. [17] in the absence or presence of 50 nM Bgtx,. Media was changed daily with drug application [18]. Media change alone was performed on the control group. At 72 hours, cells were lysed and proteins solubilized using a 0.1% Triton X-100 buffer (Triton X-100, 1 M Tris HCl, 1.5 M NaCl, 0.25 M EDTA, and 10% glycerol, in the presence of protease inhibitors (Complete Mini, Roche) as described in Nordman et al. [19]. Protein concentration was determined using a Bradford assay.

Cell viability

We tested viability in SH-SY5Y cultured cells at the end of the 72-hour treatment using the trypan blue method [20]. Cells were counted using a hemocytometer, and percent viable cells were calculated across treatment conditions relative to control.

Mitochondrial membrane potential

SH-SY5Y cells were plated on 96-well plates (Cellvis, P-96-1-N) coated with 100 μg/ml poly-D-lysine (Millipore, A-003-E) in culture media for 24 hours before amyloid application. At 72 hours, cells were incubated with 50 nM tetramethyl rhodamine, ethyl ester, perchlorate (TMRE) (Thermo Fisher Scientific, Waltham, MA, USA, T669) for 30 minutes then washed with phosphate buffered solution (PBS). TMRE fluorescence was measured using a Zeiss LSM 800 scanning-laser confocal microscope at 561 nm/595 nm excitation/emission settings. Fluorescence intensities for over 20 regions of interest (ROI) per condition were quantified using ImageJ.

Liquid-chromatography electrospray ionization mass spectrometry

Solubilized proteins samples were treated with acetone on ice for 5 minutes prior to centrifugation to precipitate proteins. The protein pellet was denatured, reduced, and alkylated with 8 M urea, 1 M dithiothreitol, 0.5 M iodoacetamide. Proteins were digested in 2 μl (0.5 μg/μl) trypsin in 500nM ammonium bicarbonate, then incubated at 37˚C for 5 h. After desalting with C-18 ZipTips (Millipore), the samples were dehydrated in a SpeedVac for 18 minutes and reconstituted in 0.1% formic acid for a final volume of 20 μl which was used to provide 3 technical replicates for liquid-chromatography electrospray ionization mass spectrometry (LC-ESI MS/MS). LC-ESI MS/MS was performed using an Exploris Orbitrap 480 equipped with an EASY-nLC 1200HPLC system (Thermo Fischer Scientific, Waltham, MA, USA). Peptides were separated using a reverse-phase PepMap RSLC 75 μm i.d by 15 cm long with a 2 μm particle size C18 LC column (Thermo Fisher Scientific, Waltham, MA, USA), eluted with 0.1% formic acid and 80% acetonitrile at a flow rate of 300 nl/min. Following a full scan at 60,000 resolving power from 300 m/z to 1200 m/z, peptides were fragmented by high-energy collision dissociation (HCD) with a normalized collision energy of 28%. EASY-IC filters for internal mass calibration, monoisotopic precursor selection, and dynamic exclusions (20 s) were enabled. Peptide precursor ions with charge states from +2 to + 4 were included.

Protein quantification and statistical analysis

Proteins were identified by comparing raw MS peptide spectra to the NCBI human protein database using SEQUEST HT search engine within the Proteome Discoverer *v2.4* (Thermo Fisher Scientific, Waltham, MA, USA) using the following parameters: mass tolerance for precursor ions = 2 ppm; mass tolerance for fragment ions = 0.05 Da; and cut-off value for the false discovery rate (FDR) in reporting peptide spectrum matches (PSM) to the database = 1%. Peptide abundance ratio was obtained by precursor ion quantification in Proteome Discoverer *v*2.4, using the vehicle control group as the denominator. Abundance ratios with adjusted p-values < 0.05 determined using a one-way analysis of variance (ANOVA) followed by Benjamini-Hochberg post-hoc analyses were considered statistically significant. Proteins were included for further analysis when matches were found in at least 2 of the 3 replicates with a recorded group abundance. Statistical significance of Gene Ontology (GO) pathways analyzed in Database for Annotation, Visualization, and Integrated Discovery (DAVID) was obtained using a Fisher Exact Test (EASE score) followed by Benjamini-Hochberg correction [21, 22].

GO enrichment analysis

To perform GO enrichment analyses on the two proteomes ("$A\beta_{42}{}^{P}$" and "$A\beta_{42}$/Bgtx ^{P}") the official gene symbols (HUGO Gene Nomenclature Committee (HGNC)) of proteins with statistically significant (adjusted p-value < 0.05) abundance ratios were uploaded to DAVID (December 2021). The "ΔP" proteome was deduced based on at least one of two criteria: 1) When the $A\beta_{42}$ and Bgtx co-treatment condition is found to result in an opposite abundance ratio measure from the $A\beta_{42}$ treatment condition alone; 2) When the $A\beta_{42}{}^{P}$ abundance ratio measure is returned to control in by $A\beta_{42}$+Bgtx co-treatment.

$$\uparrow A\beta_{42}{}^{P} \& \downarrow A\beta_{42}/\text{Bgtx} + \downarrow A\beta_{42}{}^{P} \& \uparrow A\beta_{42}/\text{Bgtx} + A\beta_{42}{}^{P} (p < 0.05) \& A\beta_{42}/\text{Bgtx} (p \geq 0.05) \quad (1)$$

GO terms were considered enriched in the uploaded dataset after the Fisher Exact Test followed by Benjamini post-hoc analysis resulted in an adjusted p-value < 0.05. Data was organized and figures presented using R statistical packages including ggplot2 [23], tidyverse [24],

GOPlot [25], and Venn.Diagram [26]. K-clustering analysis and its visualization were made using Python.

Results

Identification of an $A\beta_{42}$ responsive proteome in human neural SH-SY5Y cells

$A\beta_{42}$ neurotoxicity has been shown to involve multiple signaling pathways through various cellular entry points including cell surface receptors [27]. Recently, we used a proteomic approach to determine the impact of $A\beta_{42}$ exposure in NGF differentiated PC12 cells [14]. We extend this effort to examine proteomic responses to $A\beta_{42}$ in the human SH-SY5Y neuroblastoma cell line, which is widely used as in the study of amyloid toxicity and regulation [28]. SH-SY5Y cells were treated with 100 nM $A\beta_{42}$ prepared in a manner that has been established to favor the formation of pathogenic oligomers [17]. After 72 hours of exposure, cells were processed and analyzed using liquid chromatography electrospray ionization (LC-ESI) tandem mass spectrometry (MS/MS). SH-SY5Y cells grown under the same condition but exposed to the vehicle (media) were used as the experimental control. Whole cell proteomic analysis based on LC-ESI-MS/MS proteomic spectra identification and relative protein quantification was obtained using a label-free precursor ion quantification method [29]. The experimental design and workflow of the study are summarized in Fig 1.

We examined the potential for toxicity in our treatment condition using trypan blue. Based on a count of viable cells across all treatment conditions (100 nM $A\beta_{42}$, 100 nM $A\beta_{42}$ + 50 nM Bgtx, or 100 nM $A\beta_{rev}$) relative to control, our 72-hour drug treatment was not associated with cell toxicity (S1 Fig in S1 File). Based on an analysis of the abundance ratio measures in $A\beta_{42}$ treated cells relative to controls we identified significantly altered proteins of the $A\beta_{42}$ proteome ($A\beta_{42}^{P}$). MS/MS analysis shows that of the 4706 proteins detected within our SH-SY5Y cell fraction samples, 139 proteins were found to be significantly altered (p value < 0.05) with 58% upregulated and 42% downregulated (Fig 2A) (S1 Table in S1 File). We examined the

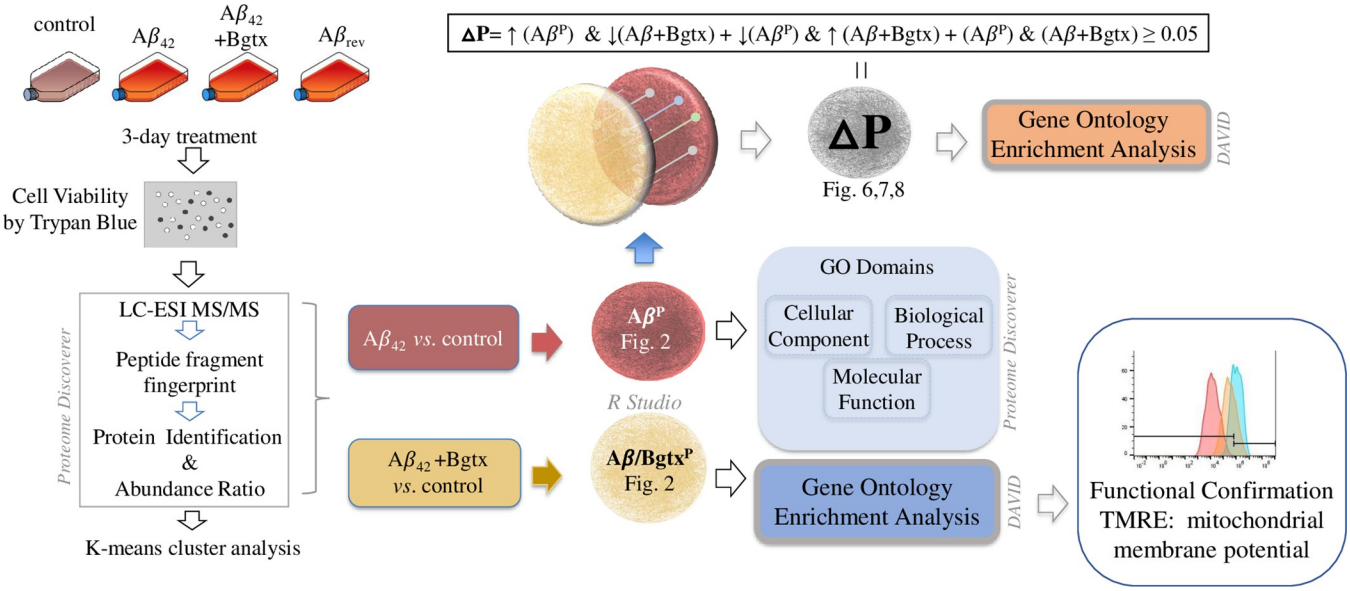

Fig 1. A summary of the experimental design and analyses. A workflow schematic showing the treatment conditions and briefly describing the mass spectrometry and bioinformatic analyses performed.

https://doi.org/10.1371/journal.pone.0270479.g001

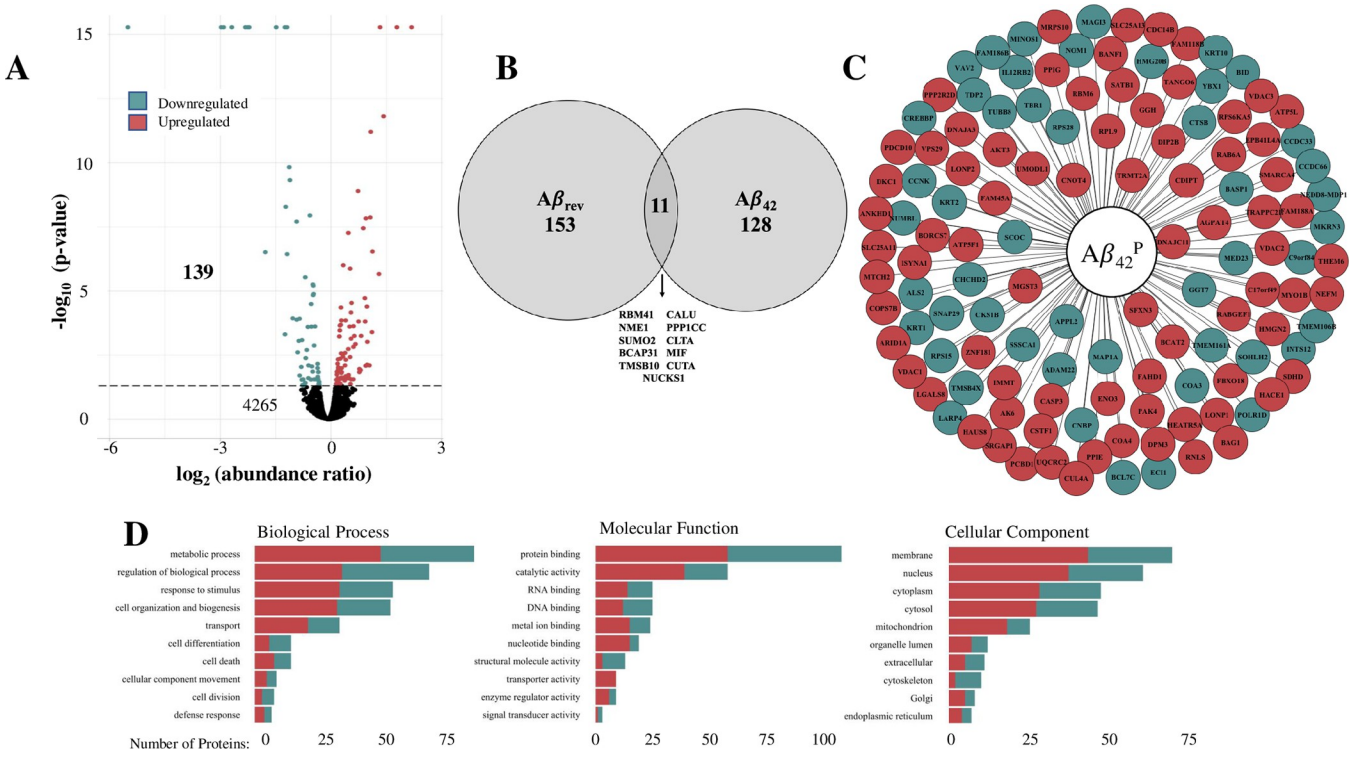

Fig 2. Proteome response to Aβ$_{42}$ treatment. A) The distribution and number of detected proteins within samples of Aβ$_{42}$ treated cells. The horizontal line indicates the threshold for statistical significance ($p < 0.05$). B) Proteins altered by Aβ$_{42}$ and Aβ$_{rev}$. C) Components of the Aβ$_{42}^{P}$ identified by their gene symbols. D) The number of proteins within the Aβ$_{42}^{P}$ associated with GO terms.

https://doi.org/10.1371/journal.pone.0270479.g002

specificity of Aβ$_{42}$ associated proteomic changes by performing matched experiments in cells using a reverse sequence peptide, Aβ$_{rev}$. As shown in Fig 2B, 72-hour treatment with Aβ$_{rev}$ was found to promote proteomic responses markedly different from Aβ$_{42}$. The full Aβ$_{rev}$ associated proteome is included in S2 Table in S1 File. A comparison of the two proteomes (Aβ$_{42}$ *vs.* Aβ$_{rev}$) indicates 11 common proteins that were excluded from the analysis. The components of the Aβ$_{42}^{P}$ are presented in Fig 2C according to their HGNC symbol, and associated Gene Ontology (GO) terms identified using Proteome Discoverer *v*2.4. The results suggest the involvement of metabolic processes, protein binding, and membrane components within Aβ$_{42}^{P}$ (Fig 2D).

Previous articles show that Aβ$_{42}$ binds to the α7 nAChR and drives neurotoxicity [30]. We tested the effect of the α7 nAChR antagonist Bgtx on Aβ$_{42}$ associated proteome modification within SH-SY5Y cells. In these experiments, cells were treated with 100 nM Aβ$_{42}$ in the presence of 50 nM Bgtx for 72 hours followed by MS/MS analysis to identify the Aβ$_{42}$ + Bgtx proteome (Aβ$_{42}$/Bgtx^{P}). As shown in Fig 3B and 3C, proteomic analysis indicates 178 significantly altered proteins within Aβ$_{42}$/Bgtx^{P} (S3 Table in S1 File). This proteome consists of 61% upregulated and 29% downregulated proteins in Fig 3B. GO analysis highlights the involvement of metabolic processes, protein binding, and membrane components within Aβ$_{42}$/Bgtx^{P} (Fig 3A) similar to Aβ$_{42}^{P}$. A comparison of the Aβ$_{42}^{P}$ and Aβ$_{42}$/Bgtx^{P} datasets indicates the presence of 67 (27%) common proteins (Fig 3D).

We performed K-means clustering analysis on proteins detected across treatment conditions (Fig 1). As shown in Fig 4A, a K-means cluster analysis shows log-transformed abundance ratios in the Aβ$_{42}$ alone relative to Aβ$_{42}$ + Bgtx treatment, with 4 cluster means indicated

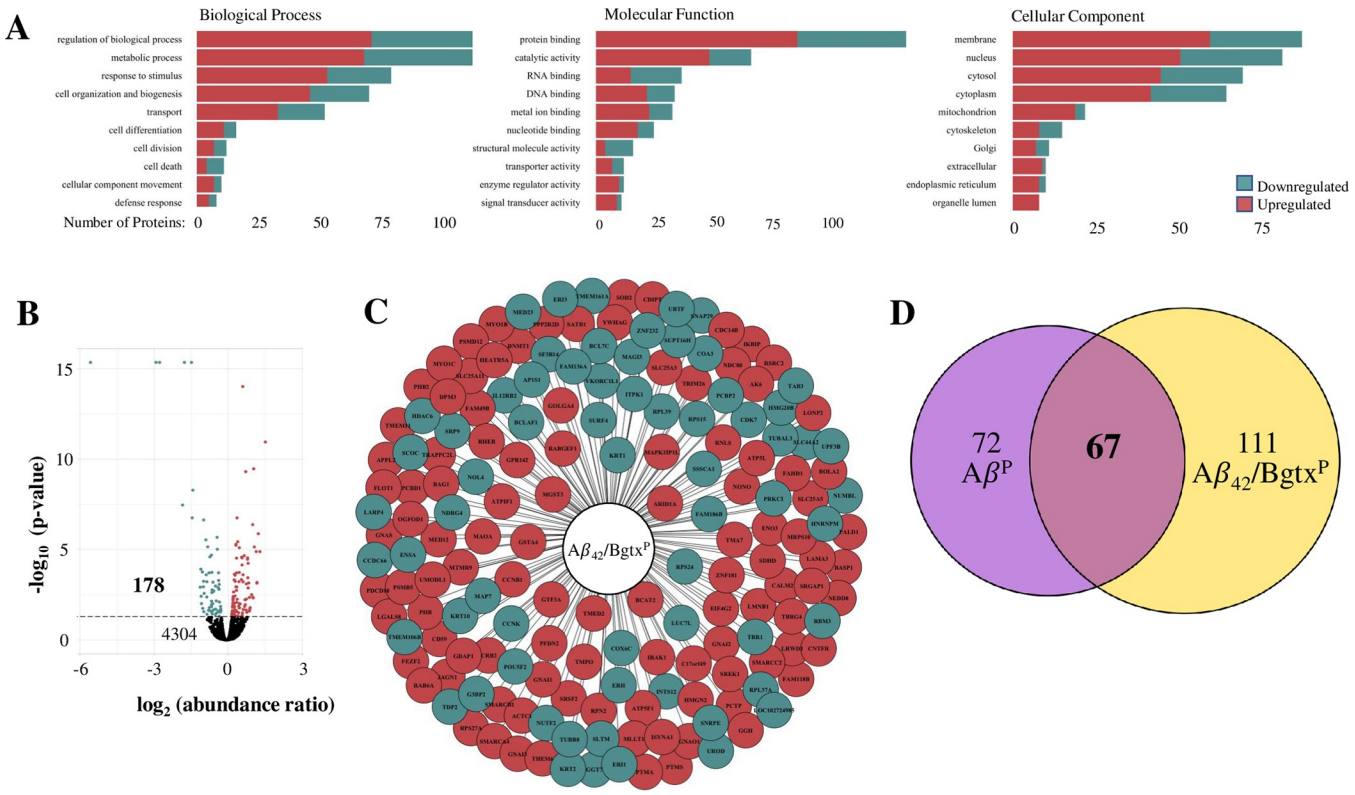

Fig 3. Proteome response to Aβ$_{42}$ + Bgtx co-treatment. A) The number of proteins within the Aβ$_{42}$/Bgtx^{P} associated with GO terms. B) The distribution and number of detected proteins within Aβ$_{42}$ + Bgtx treated cells. The horizontal line indicates the threshold for statistical significance ($p < 0.05$). C) Components of the Aβ$_{42}$/Bgtx^{P} identified by gene symbols. D) The number of proteins within the Aβ$_{42}{}^{P}$ and Aβ$_{42}$/Bgtx^{P} datasets. 67 proteins are found in both.

https://doi.org/10.1371/journal.pone.0270479.g003

across data points. We then examined the extent of similarity in protein change within Aβ$_{42}{}^{P}$ and Aβ$_{42}$/Bgtx^{P} by plotting the log transformed abundance ratio for each of the two proteomes and then determining a correlation coefficient. As shown in Fig 4B, a strong correlation ($r = 0.945$) was seen between Aβ$_{42}{}^{P}$ and Aβ$_{42}$/Bgtx^{P} suggesting that most proteins are similarly impacted across both datasets.

GO analysis of amyloid and nicotinic receptor proteomic mechanisms

Important changes in cell growth and function are driven by dynamic adaptations within gene to protein regulatory networks [31, 32]. These changes can be examined qualitatively and quantitatively using various "omic" methods in conjunction with bioinformatic analysis tools [33, 34]. To determine differences within proteomes, we performed enrichment analyses in DAVID on Aβ$_{42}{}^{P}$ and Aβ$_{42}$/Bgtx^{P} (December 2021). As shown in Fig 5, both Aβ$_{42}{}^{P}$ and Aβ$_{42}$/Bgtx^{P} appear to share key GO terms, while also distinctly associated with varied GO components. For example, mitochondria and mitochondrial processes both appear as GO terms in the DAVID enrichment analysis in Aβ$_{42}{}^{P}$, yet guanine nucleotide signaling (e.g., heterotrimeric G proteins) *only* appears in the Aβ$_{42}$/Bgtx^{P} analysis. Similarly, cytosolic and nuclear proteins feature in Aβ$_{42}$/Bgtx^{P} but are not identified within the Aβ$_{42}{}^{P}$. Within Aβ$_{42}{}^{P}$ and Aβ$_{42}$/Bgtx^{P}, protein binding, poly(A) RNA binding, nucleoplasm, and membrane are similarly enriched.

Based on the finding that Aβ$_{42}$ can bind to the α7 nAChR via the orthosteric binding site [35], we tested the effect of receptor antagonism on the Aβ$_{42}$ driven proteomic responses. We

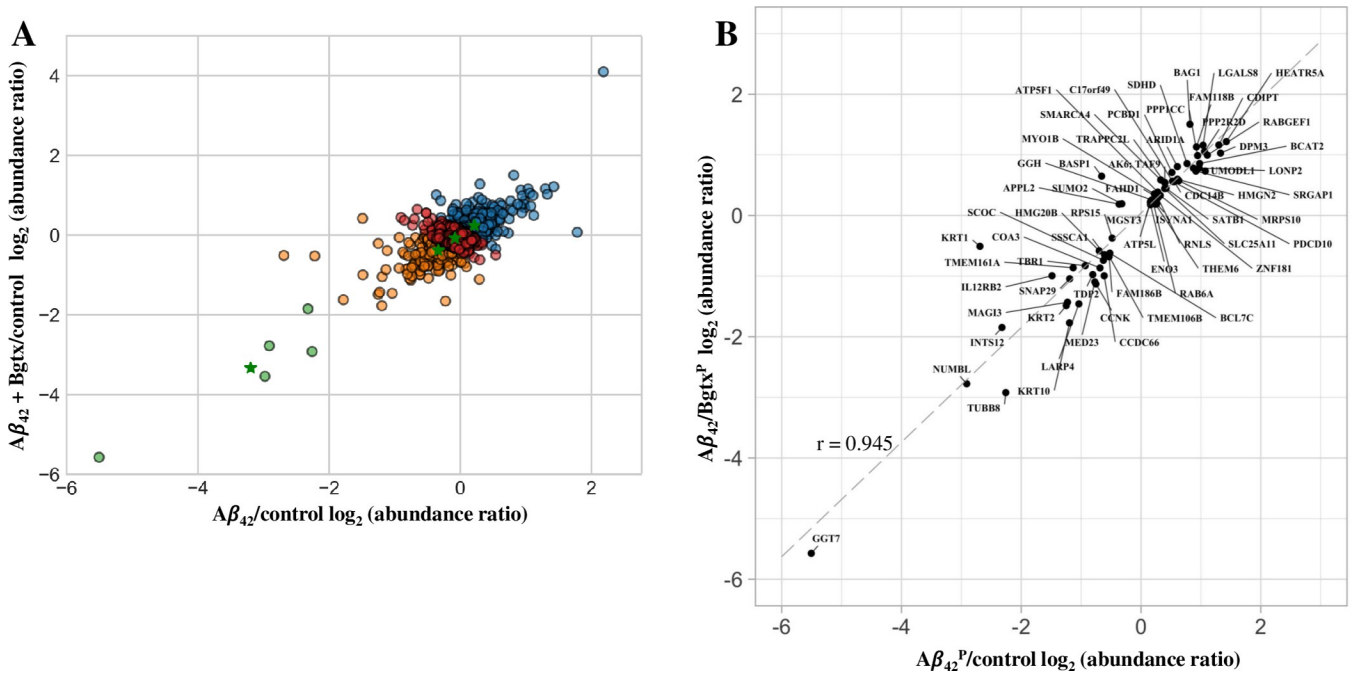

Fig 4. Clustering and correlation analysis of the proteomes. A) A K-means cluster analysis of detected proteins across both $A\beta_{42}$ and $A\beta_{42}$ + Bgtx treatment conditions. The analysis indicates 4 cluster means (green stars). B) Scatterplot and correlation analysis of the $\log_2$ transformed abundance ratio measures for individual proteins within $A\beta_{42}{}^{P}$ and $A\beta_{42}/Bgtx^{P}$.

https://doi.org/10.1371/journal.pone.0270479.g004

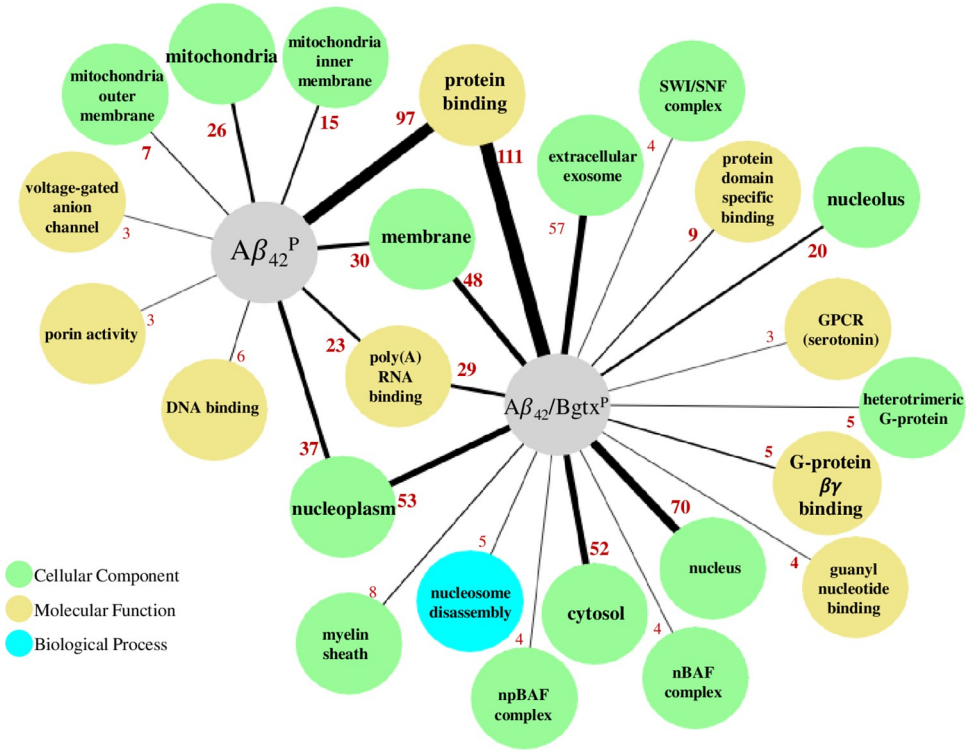

Fig 5. DAVID enrichment analysis of Aβ42P and Aβ/Bgtx^{P}. GO terms associated with $A\beta_{42}{}^{P}$ and $A\beta_{42}/Bgtx^{P}$. The number of proteins associated with each GO term are indicated by edge width and red lettering.

https://doi.org/10.1371/journal.pone.0270479.g005

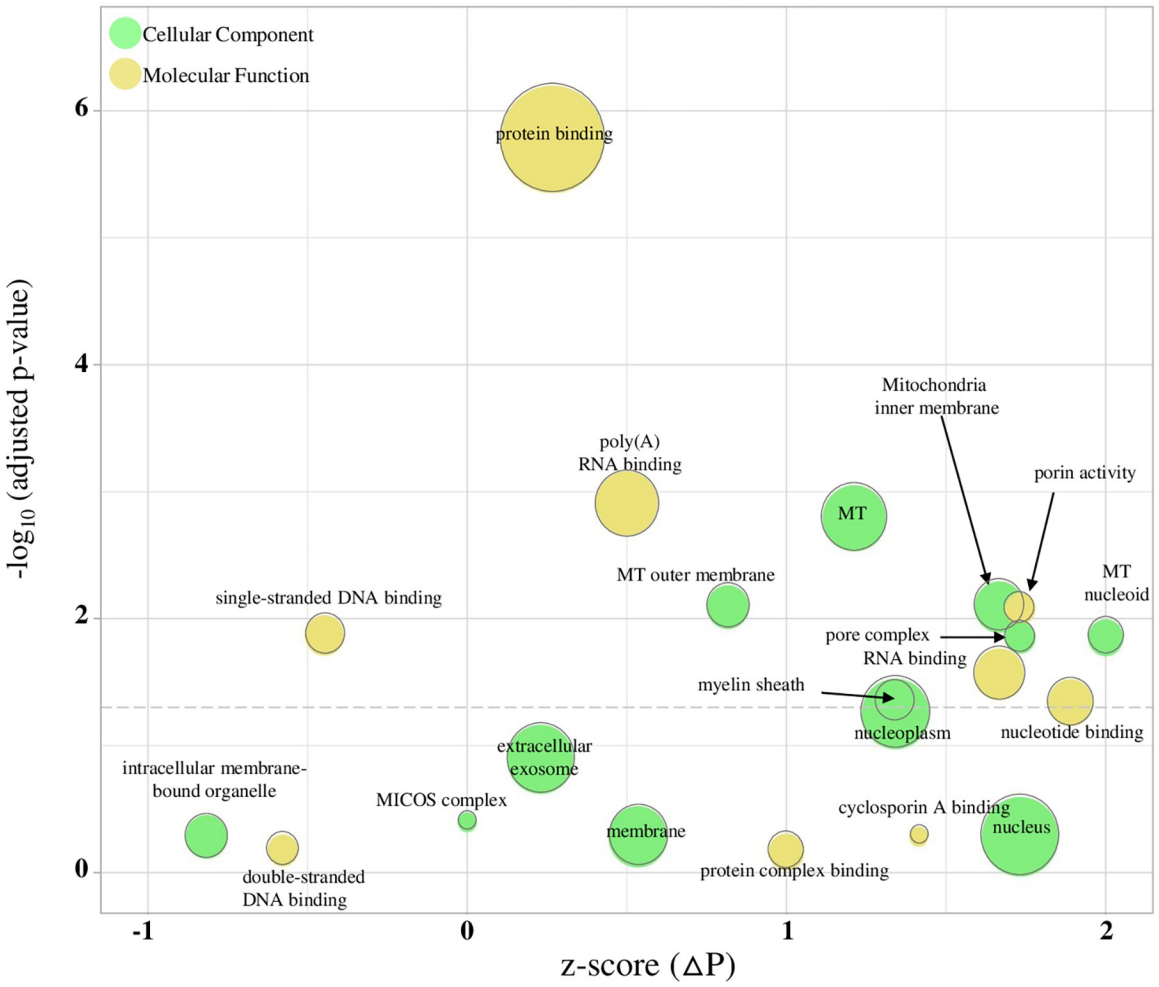

Fig 6. DAVID enrichment analysis of the ΔP proteome. ΔP was identified using the parameters indicated in Fig 1A plot of the DAVID enrichment analysis in which the bubble size describes the number of proteins within ΔP associated with each term. The x-axis is a GOPlot calculated z-score that indicates whether the term is likely increased ($z > 0$) or decreased ($z < 0$) based on the $\log_2$ abundance ratios of the proteins within the GO term. Terms that fall below the dotted grey line do not reach statistical significance as determined by an adjusted p-value ≥ 0.05 by Benjamini-Hochberg correction.

https://doi.org/10.1371/journal.pone.0270479.g006

explored this by determining which proteins within $A\beta_{42}{}^{P}$ are returned to control baseline or are altered in an opposite direction by $A\beta_{42}$ + Bgtx co-treatment. Proteins identified using this criterion are designated ΔP (Fig 1) and are listed in S4 Table in S1 File. DAVID enrichment was also used to analyze ΔP (December 2021). As shown in Fig 6, protein binding, mitochondria, and poly(A) RNA binding GO terms significantly overlap with ΔP, suggesting a role for α7nAChR in these amyloid related responses.

Nicotinic receptors impact mitochondria and protein binding components of the proteome

DAVID analyses of ΔP suggests that "protein binding" relates $A\beta_{42}$ and α7 nAChR proteome responses (Fig 7). Protein binding is a broad functional category however encompassing diverse proteins and processes that participate in interactions between not only proteins, but also proteins and other molecules including lipids and nucleic acids [36, 37]. A list of the proteins within the protein binding category from ΔP is presented in Fig 7. Quantitative changes

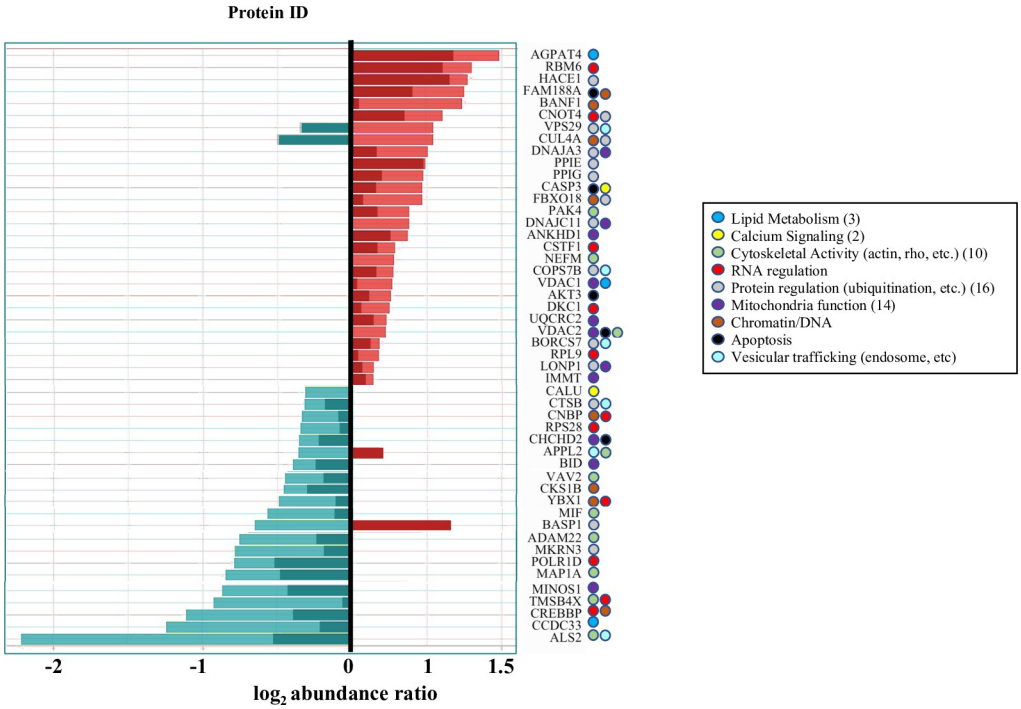

Fig 7. Protein binding components of ΔP. A change in protein levels measured by the $\log_2$ abundance ratio measures within the $A\beta_{42}$ and $A\beta_{42}$ + Bgtx treatment conditions. Color shading highlights the impact of treatment condition on protein expression. Light ($A\beta_{42}$); dark ($A\beta_{42}$ + Bgtx). The function of each protein is shown using colored dots.

https://doi.org/10.1371/journal.pone.0270479.g007

are shown for each according to the treatment condition. A classification of each protein according to its function or subcellular localization based on UniProt is indicated. This classification shows the involvement of ΔP components in various cellular processes including mitochondria, cytoskeleton, and vesicular regulation. It is interesting to note that some proteins were found to be altered in the opposite direction by $A\beta_{42}$ + Bgtx co-application relative to $A\beta_{42}$ alone.

We found a subset of proteins that decreased in the presence of $A\beta_{42}$ yet increased in the presence of $A\beta_{42}$ + Bgtx. This includes: brain acidic soluble protein1 (BASP1), which regulates actin dynamics during axon growth [38, 39]; adaptor protein, phosphotyrosine interacting with PH domain and leucine zipper 2 (APPL2), an anchor proteins in endosomes [40]. Two other proteins were increased in the presence of $A\beta_{42}$, but their expression was reduced in cells treated with $A\beta_{42}$ + Bgtx: vacuolar protein sorting-associated protein 29 (VPS29) and cullin-4A (CUL4A). VPS29 is important in endo-lysosomal trafficking, a process impacted in both Parkinson's and Alzheimer's diseases [41]. CUL4A ubiquitin ligase activity regulates protein activity in favor of $A\beta_{42}$ oligomerization [42].

Studies have shown that mitochondrial trafficking, metabolic activity, and calcium management are impacted during amyloid toxicity [43–45]. DAVID analysis of ΔP corroborates these findings and suggests the involvement of α7 nAChR in $A\beta_{42}$ mitochondrial stress. The mitochondrial proteins within ΔP are shown in Fig 8A. The figure also indicates their mitochondrial location and quantitative change according to the treatment condition. Thus, our proteomic findings highlight the impact of $A\beta_{42}$ treatment on mitochondria function through specifically altered proteins. To functionally test this, we used TMRE (cell permeant fluorescent dye used to measure mitochondrial membrane potential) to examine differences between cells treated for 72 hours with $A\beta_{42}$ or $A\beta_{42}$ + Bgtx and controls. The results show a significant

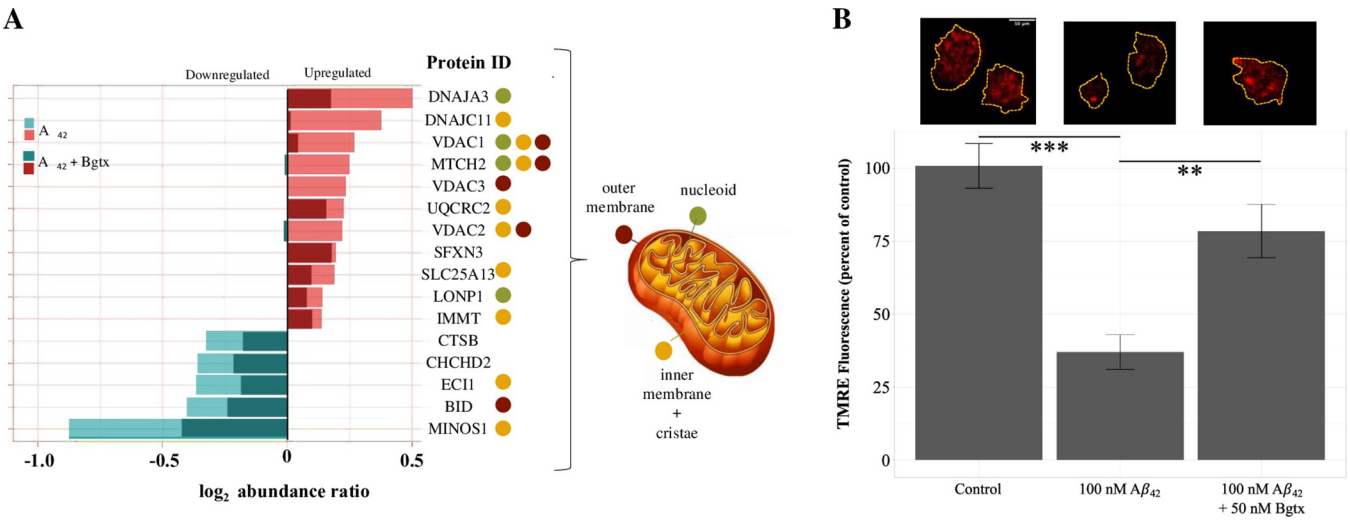

Fig 8. Mitochondrial proteins within ΔP. A) A change in protein level measured by the $\log_2$ abundance ratio measures within $A\beta_{42}$ and $A\beta_{42}$ + Bgtx treatment conditions. Color shading highlights the impact of treatment on protein expression. Light ($A\beta_{42}$); dark ($A\beta_{42}$ + Bgtx). The known localization of each protein within the mitochondria is shown using colored dots. B) Top, representative images for each condition showing fluorescence intensity of TMRE. Bottom, average percent change in TMRE fluorescence. ($n \leq 21$). $^{*}p < 0.05$; $^{**}p < 0.01$; $p < 0.001$.

https://doi.org/10.1371/journal.pone.0270479.g008

reduction in TMRE fluorescence in the $A\beta_{42}$ group ($p = 8 \times 10^{-7}$) but not in $A\beta_{42}$ + Bgtx ($p = 0.106$) when compared to the controls (Fig 8B). In addition, we found a significant reduction in TMRE fluorescence between the $A\beta_{42}$ and $A\beta_{42}$ + Bgtx treatment groups ($p = 0.001$). Given that TMRE is a measure of mitochondrial membrane potential and bioenergetic function, these results suggest that $A\beta_{42}$ exposure directly impacts mitochondrial activity in a manner that involves the α7 nAChR.

Discussion

Amyloid plaques and tau aggregates are physical components of chronic neurodegeneration considered drivers of cognitive decline in AD [1]. It is widely accepted however, that cellular and synaptic dysfunction arise earlier than the emergence of clinical disease and/or the detection of amyloid plaques due to yet unknown processes that may involve amyloid protein processing and/or accumulation [46]. Paradoxically, $A\beta_{42}$ containing plaques are seen in aging individuals without dementia, and also arise in response to brain trauma and stroke [47]. Thus, how amyloid processing leads to neurotoxicity in the course of AD remains unknown.

Soluble forms of the cleaved APP protein include the $A\beta_{42}$ peptide, are known to have neurotoxic effects in cells as well as brain slices [48]. In fact, $A\beta_{42}$ peptides alone can form highly stable oligomers (>50 kDa) that trigger tau disruptions [49]. It is well documented that $A\beta_{42}$ promotes damage to neurons through oxidative stress, membrane ion permeability, and excitotoxicity. The identification of various cellular targets of $A\beta_{42}$ including the α7 nAChR enables a framework for understanding and potentially treating amyloid toxicity in brain [10, 50, 51]. In one scenario, α7 nAChR binding has been shown to participate in the internalization and accumulation of $A\beta_{42}$ in cholinergic neurons [48].

We utilized a proteomics approach to identify mechanisms of $A\beta_{42}$ pathogenicity in the human neural SH-SY5Y cell line, which is a model for cholinergic degeneration and endogenously expresses *α7* nAChRs that bind $A\beta_{42}$ [11, 52, 53]. We compared the effects of $A\beta_{42}$ treatment alone with $A\beta_{42}$ co-applied with the selective α7 nAChR blocker, Bgtx, for 72 hours. This time course was chosen for an ability to examine proteome responses that can lead to

neurotoxicity. The overall profile of proteins identified by MS in this study appear broadly comparable between the two treatment conditions ($A\beta_{42}$ *vs*. $A\beta_{42}$+Bgtx) as evidenced by their strong correlation. This observation suggests that $A\beta_{42}$ is the dominant driver of proteomic change within these cells, and that it is possible that $A\beta_{42}$-induced changes are mediated by several receptor pathways in these cells. Indeed SH-SY5Y cells express N-methyl-D-aspartate receptors (NMDAR), which are known to interact with $A\beta_{42}$ [11]. It is noteworthy however that the cellular and molecular components of the response identified by bioinformatics points to proteomes enriched in differing GO terms. These differences underscore the actions of $A\beta_{42}$ on pathways differentially impacted by Bgtx.

A bioinformatic analysis of the proteomic data shows that $A\beta_{42}^{P}$ is enriched in mitochondrial proteins confirming the involvement of mitochondria in $A\beta_{42}$ pathogenicity [54]. Changes in specific mitochondrial proteins such as caspase 3 (CASP3) and BH3 interacting domain death agonist (BID) can contribute to apoptosis in the AD brain [55, 56]. In addition, CASP3 is known to cleave tau in a manner that encourages tangle formation consistent with findings that $A\beta_{42}$ can trigger tau disruption in neurons [57]. Our proteomic results show that Bgtx co-application diminishes the effect of $A\beta_{42}$ on several mitochondrial proteins including BID suggesting that α7 nAChRs are involved in amyloid associated mitochondrial dysfunction [58]. Experimental TMRE findings support this and confirm that α7 nAChR blockade with Bgtx significantly diminished the effect of $A\beta_{42}$ on mitochondrial membrane depolarization.

Enrichment analysis of the $A\beta_{42}$ + Bgtx co-treatment condition enabled the identification of the $A\beta_{42}$/$Bgtx^{P}$ proteome, which was different from $A\beta_{42}^{P}$. In particular, $A\beta_{42}$/$Bgtx^{P}$ is enriched in heterotrimeric G-protein components consistent with our earlier findings on nAChR signaling through various G-proteins [12, 59]. Proteomic evidence now suggests a role for G-protein activity in nAChR mediated $A\beta_{42}$ responses [12, 13]. This is consistent with findings by Lasala, et al. that indicate that $A\beta_{42}$ exposure can elicit direct conformational changes in the α7 nAChR which may thus affect its association with G-proteins in neural cells [60].

Along these lines, an enrichment analysis of the ΔP dataset was used to identify specific pathways that may functionally uncouple $A\beta_{42}$ from α7 nAChR in SH-SY5Y cells. ΔP represents proteins that are returned to baseline (control) levels or are impacted in the opposite direction in response to Bgtx co-presentation. Analysis of ΔP using DAVID enrichment identifies changes in protein binding for a wide range of cellular targets. Protein complex formation (ETC Complex I), protein synthesis and degradation, and components of cytoskeletal activity are all noted within the ΔP protein network. APPL2 is an endosomal membrane anchor protein that participates in β-catenin and PI3K/Akt signaling pathways in neurite growth [40, 61] and chromatin remodeling [44]. Trafficking in the endo- and lysosomal pathways, which has been implicated in AD and other neurodegenerative disease [62], appears linked to ΔP components through several proteins including the retromer complex that includes vacuolar sorting protein 29 (VSP29). In our data, VSP29, a protein necessary for appropriate synaptic transmission [41], is found to be upregulated in the presence of $A\beta_{42}$ but downregulated in the presence of Bgtx.

Supporting information

S1 File.
(ZIP)

Author Contributions

Conceptualization: Patricia Sinclair, Nadine Kabbani.

Data curation: Patricia Sinclair.

Formal analysis: Patricia Sinclair.

Funding acquisition: Nadine Kabbani.

Investigation: Nadine Kabbani.

Methodology: Patricia Sinclair, Nadine Kabbani.

Project administration: Nadine Kabbani.

Supervision: Nadine Kabbani.

Visualization: Patricia Sinclair, Nadine Kabbani.

Writing – original draft: Patricia Sinclair, Nadine Kabbani.

Writing – review & editing: Nadine Kabbani.

References

1. Braak H, Braak E. Neuropathological stageing of Alzheimer-related changes. Acta Neuropathol. 1991; 82(4):239–59. https://doi.org/10.1007/BF00308809 PMID: 1759558
2. Giri M, Zhang M, Lü Y. Genes associated with Alzheimer's disease: an overview and current status. Clin Interv Aging. 2016; 11:665–81. https://doi.org/10.2147/CIA.S105769 PMID: 27274215
3. Pike CJ, Walencewicz AJ, Glabe CG, Cotman CW. In vitro aging of beta-amyloid protein causes peptide aggregation and neurotoxicity. Brain Res. 1991 Nov 1; 563(1–2):311–4. https://doi.org/10.1016/0006-8993(91)91553-d PMID: 1786545
4. Maina MB, Bailey LJ, Doherty AJ, Serpell LC. The Involvement of Aβ42 and Tau in Nucleolar and Protein Synthesis Machinery Dysfunction. Front Cell Neurosci. 2018; 12:220. https://doi.org/10.3389/fncel.2018.00220 PMID: 30123109
5. Salehi A, Delcroix JD, Belichenko PV, Zhan K, Wu C, Valletta JS, et al. Increased App Expression in a Mouse Model of Down's Syndrome Disrupts NGF Transport and Causes Cholinergic Neuron Degeneration. Neuron [Internet]. 2006 Jul [cited 2021 May 12]; 51(1):29–42. Available from: https://linkinghub.elsevier.com/retrieve/pii/S0896627306004144 PMID: 16815330
6. Counts SE, He B, Che S, Ikonomovic MD, DeKosky ST, Ginsberg SD, et al. Alpha7 nicotinic receptor up-regulation in cholinergic basal forebrain neurons in Alzheimer disease. Arch Neurol. 2007 Dec; 64(12):1771–6. https://doi.org/10.1001/archneur.64.12.1771 PMID: 18071042
7. Liu AKL, Chang RCC, Pearce RKB, Gentleman SM. Nucleus basalis of Meynert revisited: anatomy, history and differential involvement in Alzheimer's and Parkinson's disease. Acta Neuropathologica [Internet]. 2015 Apr [cited 2018 Apr 30]; 129(4):527–40. Available from: http://link.springer.com/10.1007/s00401-015-1392-5 PMID: 25633602
8. Albuquerque EX, Schwarcz R. Kynurenic acid as an antagonist of α7 nicotinic acetylcholine receptors in the brain: Facts and challenges. Biochemical Pharmacology [Internet]. 2013 Apr [cited 2020 Mar 24]; 85(8):1027–32. Available from: https://linkinghub.elsevier.com/retrieve/pii/S0006295212008003 PMID: 23270993
9. Parri HR, Hernandez CM, Dineley KT. Research update: Alpha7 nicotinic acetylcholine receptor mechanisms in Alzheimer's disease. Biochemical Pharmacology [Internet]. 2011 Oct 15 [cited 2019 Dec 28]; 82(8):931–42. Available from: http://www.sciencedirect.com/science/article/pii/S0006295211004230 PMID: 21763291
10. Hascup KN, Hascup ER. Soluble Amyloid-β42 Stimulates Glutamate Release through Activation of the α7 Nicotinic Acetylcholine Receptor. J Alzheimers Dis. 2016 May 3; 53(1):337–47. https://doi.org/10.3233/JAD-160041 PMID: 27163813
11. Elnagar MR, Walls AB, Helal GK, Hamada FM, Thomsen MS, Jensen AA. Functional characterization of α7 nicotinic acetylcholine and NMDA receptor signaling in SH-SY5Y neuroblastoma cells in an ERK phosphorylation assay. Eur J Pharmacol. 2018 May 5; 826:106–13. https://doi.org/10.1016/j.ejphar.2018.02.047 PMID: 29501870
12. King JR, Nordman JC, Bridges SP, Lin MK, Kabbani N. Identification and Characterization of a G Protein-binding Cluster in α7 Nicotinic Acetylcholine Receptors. J Biol Chem [Internet]. 2015 Aug 14 [cited 2019 Sep 8]; 290(33):20060–70. Available from: https://www.ncbi.nlm.nih.gov/pmc/articles/PMC4536413/ https://doi.org/10.1074/jbc.M115.647040 PMID: 26088141

13. Nordman JC, Kabbani N. An interaction between α7 nicotinic receptors and a G-protein pathway complex regulates neurite growth in neural cells. J Cell Sci [Internet]. 2012 Nov 15 [cited 2020 Jan 31]; 125 (22):5502–13. Available from: http://jcs.biologists.org/lookup/doi/10.1242/jcs.110379 PMID: 22956546

14. Sinclair P, Baranova A, Kabbani N. Mitochondrial Disruption by Amyloid Beta 42 Identified by Proteomics and Pathway Mapping. Cells [Internet]. 2021 Sep 10 [cited 2021 Dec 29]; 10(9):2380. Available from: https://www.mdpi.com/2073-4409/10/9/2380 https://doi.org/10.3390/cells10092380 PMID: 34572029

15. Tagai N, Tanaka A, Sato A, Uchiumi F, Tanuma SI. Low Levels of Brain-Derived Neurotrophic Factor Trigger Self-aggregated Amyloid β-Induced Neuronal Cell Death in an Alzheimer's Cell Model. Biol Pharm Bull. 2020; 43(7):1073–80. https://doi.org/10.1248/bpb.b20-00082 PMID: 32612070

16. Mairuae N, Connor JR, Buranrat B, Lee SY. Oroxylum indicum (L.) extract protects human neuroblastoma SH-SY5Y cells against β-amyloid-induced cell injury. Mol Med Rep. 2019 Aug; 20(2):1933–42. https://doi.org/10.3892/mmr.2019.10411 PMID: 31257498

17. Arora K, Cheng J, Nichols RA. Nicotinic Acetylcholine Receptors Sensitize a MAPK-linked Toxicity Pathway on Prolonged Exposure to β-Amyloid. Journal of Biological Chemistry [Internet]. 2015 Aug [cited 2021 Jun 22]; 290(35):21409–20. Available from: https://linkinghub.elsevier.com/retrieve/pii/S0021925820449099 https://doi.org/10.1074/jbc.M114.634162 PMID: 26139609

18. Forest KH, Alfulaij N, Arora K, Taketa R, Sherrin T, Todorovic C, et al. Protection against β-amyloid neurotoxicity by a non-toxic endogenous N-terminal β-amyloid fragment and its active hexapeptide core sequence. Journal of Neurochemistry [Internet]. 2018 [cited 2020 Feb 27]; 144(2):201–17. Available from: https://onlinelibrary.wiley.com/doi/abs/10.1111/jnc.14257 PMID: 29164616

19. Nordman JC, Muldoon P, Clark S, Damaj MI, Kabbani N. The α 4 Nicotinic Receptor Promotes CD4 $^{+}$ T-Cell Proliferation and a Helper T-Cell Immune Response. Mol Pharmacol [Internet]. 2014 Jan [cited 2020 Jun 23]; 85(1):50–61. Available from: http://molpharm.aspetjournals.org/lookup/doi/10.1124/mol.113.088484 PMID: 24107512

20. Strober W. Trypan Blue Exclusion Test of Cell Viability. Curr Protoc Immunol. 2015 Nov 2; 111:A3.B.1–A3.B.3. https://doi.org/10.1002/0471142735.ima03bs111 PMID: 26529666

21. Huang DW, Sherman BT, Lempicki RA. Systematic and integrative analysis of large gene lists using DAVID bioinformatics resources. Nat Protoc. 2009; 4(1):44–57. https://doi.org/10.1038/nprot.2008.211 PMID: 19131956

22. Huang DW, Sherman BT, Lempicki RA. Bioinformatics enrichment tools: paths toward the comprehensive functional analysis of large gene lists. Nucleic Acids Res. 2009 Jan; 37(1):1–13. https://doi.org/10.1093/nar/gkn923 PMID: 19033363

23. Wickham H. ggplot2: Elegant graphics for data analysis [Internet]. Springer-Verlag, New York; 2016. Available from: https://ggplot2.tidyverse.org

24. Wickham H, Averick M, Bryan J, Chang W, McGowan L, François R, et al. Welcome to the Tidyverse. JOSS [Internet]. 2019 Nov 21 [cited 2021 Dec 29]; 4(43):1686. Available from: https://joss.theoj.org/papers/10.21105/joss.01686

25. Walter W, Sánchez-Cabo F, Ricote M. GOplot: an R package for visually combining expression data with functional analysis. Bioinformatics. 2015 Sep 1; 31(17):2912–4. https://doi.org/10.1093/bioinformatics/btv300 PMID: 25964631

26. Chen H, Boutros PC. VennDiagram: a package for the generation of highly-customizable Venn and Euler diagrams in R. BMC Bioinformatics. 2011 Jan 26; 12:35. https://doi.org/10.1186/1471-2105-12-35 PMID: 21269502

27. Deng L, Haynes P, Wu Y, Amirkhani A, Kamath K, Wu J, et al. Amyloid-beta peptide neurotoxicity in human neuronal cells is associated with modulation of insulin-like growth factor transport, lysosomal machinery and extracellular matrix receptor interactions. Neural Regen Res [Internet]. 2020 [cited 2021 Dec 29]; 15(11):2131. Available from: http://www.nrronline.org/text.asp?2020/15/11/2131/282261 https://doi.org/10.4103/1673-5374.282261 PMID: 32394972

28. Mucke L, Selkoe DJ. Neurotoxicity of amyloid β-protein: synaptic and network dysfunction. Cold Spring Harb Perspect Med. 2012 Jul; 2(7):a006338. https://doi.org/10.1101/cshperspect.a006338 PMID: 22762015

29. Mehta S, Easterly CW, Sajulga R, Millikin RJ, Argentini A, Eguinoa I, et al. Precursor Intensity-Based Label-Free Quantification Software Tools for Proteomic and Multi-Omic Analysis within the Galaxy Platform. Proteomes [Internet]. 2020 Jul 8 [cited 2021 Jul 27]; 8(3):15. Available from: https://www.mdpi.com/2227-7382/8/3/15 https://doi.org/10.3390/proteomes8030015 PMID: 32650610

30. Dajas-Bailador FA, Lima PA, Wonnacott S. The alpha7 nicotinic acetylcholine receptor subtype mediates nicotine protection against NMDA excitotoxicity in primary hippocampal cultures through a Ca(2+) dependent mechanism. Neuropharmacology. 2000 Oct; 39(13):2799–807. https://doi.org/10.1016/s0028-3908(00)00127-1 PMID: 11044750

31. Engelman JA, Luo J, Cantley LC. The evolution of phosphatidylinositol 3-kinases as regulators of growth and metabolism. Nat Rev Genet. 2006 Aug; 7(8):606–19. https://doi.org/10.1038/nrg1879 PMID: 16847462

32. Merkin J, Russell C, Chen P, Burge CB. Evolutionary dynamics of gene and isoform regulation in Mammalian tissues. Science. 2012 Dec 21; 338(6114):1593–9. https://doi.org/10.1126/science.1228186 PMID: 23258891

33. Al Shweiki MR, Mönchgesang S, Majovsky P, Thieme D, Trutschel D, Hoehenwarter W. Assessment of Label-Free Quantification in Discovery Proteomics and Impact of Technological Factors and Natural Variability of Protein Abundance. J Proteome Res [Internet]. 2017 Apr 7 [cited 2021 May 12]; 16 (4):1410–24. Available from: https://pubs.acs.org/doi/10.1021/acs.jproteome.6b00645 PMID: 28217993

34. Karimpour-Fard A, Epperson LE, Hunter LE. A survey of computational tools for downstream analysis of proteomic and other omic datasets. Hum Genomics. 2015 Oct 28; 9:28. https://doi.org/10.1186/s40246-015-0050-2 PMID: 26510531

35. Cecon E, Dam J, Luka M, Gautier C, Chollet AM, Delagrange P, et al. Quantitative assessment of oligomeric amyloid β peptide binding to α7 nicotinic receptor. Br J Pharmacol. 2019 Sep; 176(18):3475–88. https://doi.org/10.1111/bph.14688 PMID: 30981214

36. Castello A, Fischer B, Eichelbaum K, Horos R, Beckmann BM, Strein C, et al. Insights into RNA biology from an atlas of mammalian mRNA-binding proteins. Cell. 2012 Jun 8; 149(6):1393–406. https://doi.org/10.1016/j.cell.2012.04.031 PMID: 22658674

37. Ostroumova OS, Schagina LV, Mosevitsky MI, Zakharov VV. Ion channel activity of brain abundant protein BASP1 in planar lipid bilayers. FEBS J. 2011 Feb; 278(3):461–9. https://doi.org/10.1111/j.1742-4658.2010.07967.x PMID: 21156029

38. Laux T, Fukami K, Thelen M, Golub T, Frey D, Caroni P. GAP43, MARCKS, and CAP23 modulate PI (4,5)P(2) at plasmalemmal rafts, and regulate cell cortex actin dynamics through a common mechanism. J Cell Biol. 2000 Jun 26; 149(7):1455–72. https://doi.org/10.1083/jcb.149.7.1455 PMID: 10871285

39. Chung D, Shum A, Caraveo G. GAP-43 and BASP1 in Axon Regeneration: Implications for the Treatment of Neurodegenerative Diseases. Front Cell Dev Biol. 2020; 8:567537. https://doi.org/10.3389/fcell.2020.567537 PMID: 33015061

40. Rashid S, Pilecka I, Torun A, Olchowik M, Bielinska B, Miaczynska M. Endosomal adaptor proteins APPL1 and APPL2 are novel activators of beta-catenin/TCF-mediated transcription. J Biol Chem. 2009 Jul 3; 284(27):18115–28. https://doi.org/10.1074/jbc.M109.007237 PMID: 19433865

41. Ye H, Ojelade SA, Li-Kroeger D, Zuo Z, Wang L, Li Y, et al. Retromer subunit, VPS29, regulates synaptic transmission and is required for endolysosomal function in the aging brain. Elife. 2020 Apr 14; 9: e51977. https://doi.org/10.7554/eLife.51977 PMID: 32286230

42. Yasukawa T, Tsutsui A, Tomomori-Sato C, Sato S, Saraf A, Washburn MP, et al. NRBP1-Containing CRL2/CRL4A Regulates Amyloid β Production by Targeting BRI2 and BRI3 for Degradation. Cell Reports [Internet]. 2020 Mar [cited 2022 Mar 31]; 30(10):3478–3491.e6. Available from: https://linkinghub.elsevier.com/retrieve/pii/S2211124720302278 https://doi.org/10.1016/j.celrep.2020.02.059 PMID: 32160551

43. Rui Y, Tiwari P, Xie Z, Zheng JQ. Acute Impairment of Mitochondrial Trafficking by β-Amyloid Peptides in Hippocampal Neurons. J Neurosci [Internet]. 2006 Oct 11 [cited 2021 May 12]; 26(41):10480–7. Available from: https://www.ncbi.nlm.nih.gov/pmc/articles/PMC6674697/ https://doi.org/10.1523/JNEUROSCI.3231-06.2006 PMID: 17035532

44. Miaczynska M, Christoforidis S, Giner A, Shevchenko A, Uttenweiler-Joseph S, Habermann B, et al. APPL proteins link Rab5 to nuclear signal transduction via an endosomal compartment. Cell. 2004 Feb 6; 116(3):445–56. https://doi.org/10.1016/s0092-8674(04)00117-5 PMID: 15016378

45. Wang W, Zhao F, Ma X, Perry G, Zhu X. Mitochondria dysfunction in the pathogenesis of Alzheimer's disease: recent advances. Mol Neurodegeneration [Internet]. 2020 Dec [cited 2021 Jun 22]; 15(1):30. Available from: https://molecularneurodegeneration.biomedcentral.com/articles/10.1186/s13024-020-00376-6 PMID: 32471464

46. Tönnies E, Trushina E. Oxidative Stress, Synaptic Dysfunction, and Alzheimer's Disease. J Alzheimers Dis. 2017; 57(4):1105–21. https://doi.org/10.3233/JAD-161088 PMID: 28059794

47. Pluta R, Ułamek-Kozioł M, Januszewski S, Czuczwar SJ. Participation of Amyloid and Tau Protein in Neuronal Death and Neurodegeneration after Brain Ischemia. Int J Mol Sci. 2020 Jun 28; 21(13): E4599. https://doi.org/10.3390/ijms21134599 PMID: 32605320

48. Fontana IC, Zimmer AR, Rocha AS, Gosmann G, Souza DO, Lourenco MV, et al. Amyloid-β oligomers in cellular models of Alzheimer's disease. Journal of Neurochemistry [Internet]. 2020 [cited 2021 Jun 9];

155(4):348–69. Available from: https://onlinelibrary.wiley.com/doi/abs/10.1111/jnc.15030 PMID: 32320074

49. Tolar M, Hey J, Power A, Abushakra S. Neurotoxic Soluble Amyloid Oligomers Drive Alzheimer's Pathogenesis and Represent a Clinically Validated Target for Slowing Disease Progression. Int J Mol Sci. 2021 Jun 14; 22(12):6355. https://doi.org/10.3390/ijms22126355 PMID: 34198582

50. Pinheiro L, Faustino C. Therapeutic Strategies Targeting Amyloid-β in Alzheimer's Disease. Curr Alzheimer Res. 2019; 16(5):418–52. https://doi.org/10.2174/1567205016666190321163438 PMID: 30907320

51. Xia M, Cheng X, Yi R, Gao D, Xiong J. The Binding Receptors of Aβ: an Alternative Therapeutic Target for Alzheimer's Disease. Mol Neurobiol [Internet]. 2016 Jan [cited 2021 Jul 11]; 53(1):455–71. Available from: http://link.springer.com/10.1007/s12035-014-8994-0 PMID: 25465238

52. Yang WN, Ma KG, Chen XL, Shi LL, Bu G, Hu XD, et al. Mitogen-activated protein kinase signaling pathways are involved in regulating α7 nicotinic acetylcholine receptor-mediated amyloid-β uptake in SH-SY5Y cells. Neuroscience. 2014 Oct 10; 278:276–90. https://doi.org/10.1016/j.neuroscience.2014.08.013 PMID: 25168732

53. Young KF, Pasternak SH, Rylett RJ. Oligomeric aggregates of amyloid β peptide 1–42 activate ERK/MAPK in SH-SY5Y cells via the α7 nicotinic receptor. Neurochemistry International [Internet]. 2009 Dec [cited 2019 Sep 8]; 55(8):796–801. Available from: https://linkinghub.elsevier.com/retrieve/pii/S019701860900237X https://doi.org/10.1016/j.neuint.2009.08.002 PMID: 19666073

54. Abramov AY, Canevari L, Duchen MR. Beta-amyloid peptides induce mitochondrial dysfunction and oxidative stress in astrocytes and death of neurons through activation of NADPH oxidase. J Neurosci. 2004 Jan 14; 24(2):565–75. https://doi.org/10.1523/JNEUROSCI.4042-03.2004 PMID: 14724257

55. Luo X, Budihardjo I, Zou H, Slaughter C, Wang X. Bid, a Bcl2 interacting protein, mediates cytochrome c release from mitochondria in response to activation of cell surface death receptors. Cell. 1998 Aug 21; 94(4):481–90. https://doi.org/10.1016/s0092-8674(00)81589-5 PMID: 9727491

56. Zhivotovsky B, Samali A, Gahm A, Orrenius S. Caspases: their intracellular localization and translocation during apoptosis. Cell Death Differ [Internet]. 1999 Jul [cited 2020 Feb 25]; 6(7):644–51. Available from: http://www.nature.com/articles/4400536 https://doi.org/10.1038/sj.cdd.4400536 PMID: 10453075

57. de Calignon A, Fox LM, Pitstick R, Carlson GA, Bacskai BJ, Spires-Jones TL, et al. Caspase activation precedes and leads to tangles. Nature [Internet]. 2010 Apr 22 [cited 2019 Oct 27]; 464(7292):1201–4. Available from: https://www.ncbi.nlm.nih.gov/pmc/articles/PMC3091360/ https://doi.org/10.1038/nature08890 PMID: 20357768

58. Gergalova G, Lykhmus O, Kalashnyk O, Koval L, Chernyshov V, Kryukova E, et al. Mitochondria Express α7 Nicotinic Acetylcholine Receptors to Regulate Ca2+ Accumulation and Cytochrome c Release: Study on Isolated Mitochondria. PLOS ONE [Internet]. 2012 Feb 16 [cited 2019 Sep 17]; 7(2): e31361. Available from: https://journals.plos.org/plosone/article?id=10.1371/journal.pone.0031361 PMID: 22359587

59. King JR, Kabbani N. Alpha 7 nicotinic receptor coupling to heterotrimeric G proteins modulates RhoA activation, cytoskeletal motility, and structural growth. Journal of Neurochemistry [Internet]. 2016 [cited 2020 Jun 30]; 138(4):532–45. Available from: https://onlinelibrary.wiley.com/doi/abs/10.1111/jnc.13660 PMID: 27167578

60. Lasala M, Fabiani C, Corradi J, Antollini S, Bouzat C. Molecular Modulation of Human α7 Nicotinic Receptor by Amyloid-β Peptides. Front Cell Neurosci [Internet]. 2019 Feb 8 [cited 2019 Oct 27]; 13:37. Available from: https://www.frontiersin.org/article/10.3389/fncel.2019.00037/full PMID: 30800059

61. Mao L, Lin W, Nie T, Hui X, Gao X, Li K, et al. Absence of Appl2 sensitizes endotoxin shock through activation of PI3K/Akt pathway. Cell Biosci. 2014; 4(1):60. https://doi.org/10.1186/2045-3701-4-60 PMID: 25328665

62. Small SA, Simoes-Spassov S, Mayeux R, Petsko GA. Endosomal Traffic Jams Represent a Pathogenic Hub and Therapeutic Target in Alzheimer's Disease. Trends Neurosci. 2017 Oct; 40(10):592–602. https://doi.org/10.1016/j.tins.2017.08.003 PMID: 28962801